Universal behavior for electromagnetic interference shielding effectiveness of polymer based composite materials

C. Retailleau, J. Alaa Eddine, F. Ndagijimana, F. Haddad, Bernard Bayard, B. Sauviac, P. Alcouffe, M. Fumagalli, V. Bounor-Legaré, A. Serghei

Universal behavior for electromagnetic interference shielding effectiveness of polymer based composite materials

C. Retailleau[1], J. Alaa-Eddine[2], F. Ndagijimana[2], F. Haddad[3], B. Bayard[3], B. Sauviac[3], P. Alcouffe[1], M. Fumagalli[1], V. Bounor-Legaré[1], A. Serghei[1]

[1]*Université Claude Bernard Lyon1, IMP, CNRS-UMR 5223, 69622 Villeurbanne, France*

[2]*Université de Grenoble Alpes, Grenoble, France*

[3]*Université Jean Monnet, Laboratoire Hubert Curien, Saint-Etienne, France*

Abstract: The electromagnetic interference shielding properties and the electrical properties of poly(methylmethacrylate) (PMMA) based composite materials prepared using different types of fillers (multi-wall carbon nanotubes, carbon black, silver coated glass microfibers) have been investigated in a broad frequency range. By combining a theoretical and an experimental analysis we show that, irrespective of the nature of the conductive material (carbon based or metallic), the correlation between the electromagnetic shielding effectiveness, electrical conductivity and sample thickness follows a universal behavior, all experimental points falling onto a single universal curve predicted by our theoretical analysis. This is demonstrated not only for our own experimental results, but also for numerous experimental data reported in the scientific literature where other types of polymer matrices and other types of fillers have been investigated. The universal relationship found in our study opens the perspective of a precise predictive determination of the electromagnetic interference shielding effectiveness of composite materials based exclusively on their electrical properties.

Keywords: Electromagnetic interference shielding (EMI); Electrical properties; Polymer-matrix composites (PMCs)

1. Introduction

With the tremendous technological developments related to the accelerated growth in the field of telecommunications, our contemporary society is increasingly facing the problem of electromagnetic pollution. The electromagnetic pollution, expected to grow even faster in the coming years, leads to electromagnetic interference (EMI) phenomena that disturb the correct functioning of instruments and systems, posing thereby an important risk to industrial applications and human being. Developing technological solutions and materials for protecting instruments and systems from electromagnetic interference phenomena becomes thus a major challenge in our society. As revealed by numerous experimental and theoretical studies, the electrical conductivity represents an important physical parameter to be taken into account in order to design materials exhibiting significant shielding properties [1–4]. Generally, the shielding effectiveness of materials increases with their conductivity value due to the mechanisms of wave reflection and absorption [1,2]. For a superior shielding performance, metals are the materials of choice. However, important drawbacks related to their costs, processing, weight, rigidity, corrosion prevent them from being used in many applications where light, cheap, easy processable materials turn out to be more advantageous. Polymer based conductive composite materials [5–15] represent therefore an effective alternative in this case. In order to render a polymeric material electrically conductive, conductive fillers of different nature, size or form factor are added into the polymer matrix. Through the percolation generated by the electrical contacts and tunneling effects between the fillers, a conductive network is formed in the volume of the insulating polymer matrix leading to a conductive composite material [6,16–19]. The shielding effectiveness and the conductive properties of polymer based conductive composite materials have been investigated in numerous studies [6,10–12,19–21]. The correlation between conductivity and shielding effectiveness has been experimentally analyzed in many studies and empirical relationships between these two parameters have been demonstrated [10,11,22–27]. Theoretical studies investigating the shielding effectiveness in

dependence on the conductivity parameter have been reported as well [1,2]. However, in most of the cases, this correlation follows empirical relationships that are not applicable for all composite materials. A unifying approach able to correctly predict the shielding effectiveness of composite materials irrespective of the nature of the polymer matrix and of the nature of the employed fillers has not been validated so far. A unifying approach applicable for all polymer based composite materials would give one the possibility of precisely determining the shielding effectiveness of composite materials by taking into account the conductivity value and the sample thickness.

By combining a theoretical and an experimental analysis, here we show that the correlation between the shielding effectiveness of polymer based composite materials, their electrical conductivity and the sample thickness follow a universal relationship. All experimental points obtained in our study and in the scientific literature, using different polymer matrices and different fillers, fall onto a single collapsing curve, predicted by our theoretical analysis. The shielding performance of composite materials can be thus assessed by taken into account the material conductivity and the sample thickness. This opens the perspective of precisely predicting the shielding performance of composite materials based solely on their electrical conductivity.

2. Materials and Methods

2.1 Materials

The composite materials were prepared by melt mixing using poly(methylmethacrylate) (PMMA) as a polymer matrix (Altuglas® V 825T, supplied by Arkema) and three different types of conductive fillers: multi-wall carbon nanotubes (CNT), carbon black and silver coated glass microfibers. The CNTs, supplied by Nanocyl S.A. (NC 7000), have an average diameter of 9.5 nm, an average length of 1.5 microns, a surface area of 250-300 m^2/g and a volume resistivity of 10^{-4} Ωcm. One series of samples have been prepared by diluting a masterbatch, (PMMA/CNT

masterbatch supplied by Nanocyl and filled with 5 vol% of CNT). This has realized by adding supplementary amounts of pure PMMA during the melt-mixing process, in order to reach a target filler concentration in the final composite. A second series of PMMA/CNT composites was prepared by directly adding the CNTs into the polymer matrix during the melt-mixing. The carbon black fillers (CB, Vulcan Xcmax) were supplied Cabot Corp. The silver-coated glass microfibers (AgGF) were supplied by Hart Materials Ltd. (SF82TF20). They have an average length of 109 microns and an average diameter of 18 microns. After melt-mixing, all samples were prepared in form of plates of 1 mm thickness, by compression molding at 210 ^{o}C.

2.2 Methods

Melt-mixing: The composite materials have been prepared by melt-mixing at 210 ^{o}C, using a Haake PolyLab internal mixer (Haake™ Rheomix). The mixing process, realized by using two rotating roller rotors, was performed using a moderate rotation speed of 80 rpm. The polymer, added first, was melted and mixed until torque stabilization. Then, the fillers were incorporated into the polymer matrix and the composite was mixed until temperature and torque stabilization occurred, typically in less than 10 min. After melt-mixing, the composite was cooled down to room temperature, milled and hot-pressed at 210 ^{o}C to form plates of 1 mm thickness.

Conductivity measurements: The conductivity measurements have been carried-out between 10^6 Hz and 1 Hz using a Broadband Dielectric Spectrometer (BDS) (from Novocontrol GmbH). Low voltages, typically in the range of 0.1 V, have been applied. The contact zones between the sample and the measurement electrodes have been gold-metallized by sputtering, in order to eliminate the influence of the contact resistance.

Shielding effectiveness measurements: The shielding measurements have been carried out using a Vector Network Analyzer (2 Port Shockline VNA Anritsu, Model MS46522B) operating in the frequency range from 50 kHz to 18 GHz. Its dynamic range was superior to 90 dB

in the whole frequency range. A coaxial measurement cell (EpsiMu, Multiwave Innovation) was used to measure the S-parameters and determine the shielding effectiveness. A TOSLKF50A-20 Type K(f) calibration kit was used to calibrate the system. Before each set of measurements, the VNA was calibrated and the empty cell was measured to validate that no shielding occurs in the measured frequency range. The power was set to 0 dBm, which corresponds to 1 mW.

3. Results and Discussion

3.1 The electromagnetic interference shielding effectiveness

The EMI shielding effectiveness of a given shield is generally defined as [1,28]:

$$SE = 10\log\left|\frac{P_i}{P_t}\right| = 20\log\left|\frac{H_i}{H_t}\right| = 20\log\left|\frac{E_i}{E_t}\right| \quad [1]$$

where P_i, E_i and H_i are the power, electric field amplitude and magnetic field amplitude of the incident electromagnetic wave, and P_t, E_t and H_t the power and amplitudes of the EM wave transmitted through the shield. When an incident electromagnetic wave hits an EMI shield, several phenomena take place, as schematically illustrated in Fig 1. First, a part of the incident EM wave gets reflected at the first air/material interface and does not penetrate the material at all. This shielding mechanism is called reflection. The other part of the wave gets into the shield, goes through its thickness and undergoes electromagnetic absorption all along its path. This represents the second main shielding mechanism called absorption. The EM wave power gets dissipated and transformed into thermal energy through induced current dissipation, dielectric polarization, interfacial polarization, eddy current dissipation, hysteresis loss and magnetic resonance loss [29]. When the EM wave gets to the second material/air interface, a part of the wave goes through the interface and it is transmitted to the analyzer. The other part of the wave gets reflected back and

goes to the first interface. Along its path, it undergoes again electromagnetic absorption and gives rise to a secondary reflection at the first interface and a secondary transmitted wave and so on. This phenomenon is called multiple internal reflection. Consequently, the shielding phenomenon is determined by three major mechanisms: reflection, absorption and multiple reflections [1,2,4,7].

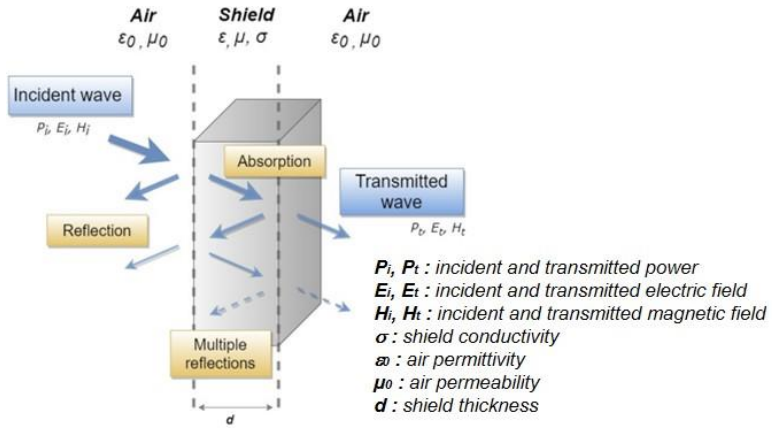

Figure 1: Schematic representation of different mechanisms for electromagnetic shielding.

The relation between the electrical conductivity and the shielding effectiveness measured using the coaxial cell can be analyzed by considering the attenuation parameter of electrical signals along a coaxial transmission line. A schematic representation of the coaxial measurement cell is represented in Fig. 2. The sample, prepared in the form of a disc of given thickness d, is connected between the inner and the outer electrode of the coaxial cell, at the junction between the two flanges. The orientation of the electric field is parallel to the surface of the sample, being thus equivalent to that of a plane electromagnetic wave penetrating the sample under normal incident angle. At low frequencies, when the wavelength of the electromagnetic wave becomes much larger than the length of the co-axial measurement circuit (on a usual laboratory scale typically bellow 100 MHz), the coaxial cell can be represented by an equivalent electrical circuit (Fig. 2c) consisting of a VNA generator, the electrical output impedance Z_C, the electrical impedance of the sample under investigation Z_L, and the input impedance Z_C of the detector.

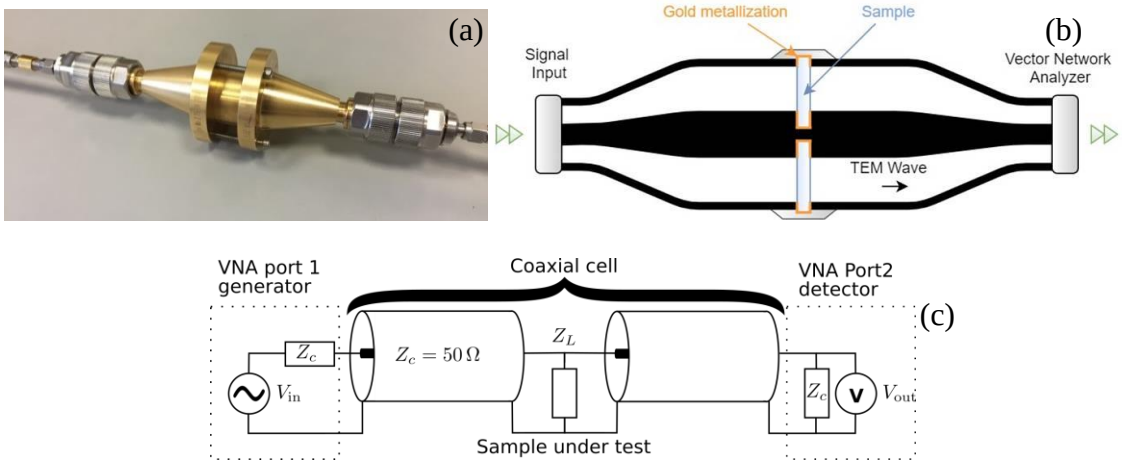

Figure 2: (a) the coaxial cell used in our study; (b) schematic representation of the coaxial measurement cell. (b) equivalent electric circuit representing a coaxial cell.

The sample impedance Z_L is measured between two concentric circular electrodes, corresponding, in the case of a dominant resistive response, to the following formula:

$$Z_L = \frac{1}{2\pi\sigma L}\ln\left(\frac{D_{out}}{D_{in}}\right) \qquad \text{(eq. 1)}$$

where σ represents the electrical conductivity of the sample, L the sample thickness, and D_{out} and D_{in} the diameter of the outer and inner electrode of the coaxial cell. The characteristic impedance of a coaxial transmission line is given by:

$$Z_C = \frac{1}{2\pi}\sqrt{\frac{\mu_0}{\varepsilon_0}}\ln\left(\frac{D_{out}}{D_{in}}\right) \cong 60\ln\left(\frac{D_{out}}{D_{in}}\right) \qquad \text{(eq. 2)}$$

According to the electrical circuit represented in Fig. 2, the transmission parameter S_{21} of electrical signals transmitted through the sample impedance Z_L [1,2,28] is given by:

$$S_{21} = \frac{|V_{\text{out}}|}{|V_{\text{in}}|} = \frac{2}{\left|2+\frac{Z_C}{Z_L}\right|} = \frac{1}{\left|1+\frac{Z_C}{2Z_L}\right|} \quad \text{(eq. 3)}$$

where V_{out} represents the electrical voltage in the presence of the sample impedance Z_L and V_{in} the electrical voltage at the end of the coaxial cell without the sample. By combining eq. 1, 2 and 3 one obtains the following formula:

$$S_{21} = \frac{1}{1+60\pi\sigma d} \quad \text{(eq. 4)}$$

This formula relates the transmission parameter S_{21} to the conductivity of the investigated material and its sample thickness. Based on the attenuation parameter measured in the coaxial line [1,2,5,28], the shielding effectiveness SE of a material is defined as:

$$SE[dB] = -20\log_{10}(S_{21}) \quad \text{(eq. 5)}$$

As demonstrated in the following, eq. 4-5 can be successfully used to quantitatively determine the shielding effectiveness of a large number of different composites based solely on their electrical conductivity and sample thickness. As revealed in numerous studies [3,5,8,9,30], significant shielding properties can be obtained by employing highly conductive materials. In this case, the sample impedance Z_L is typically in the range up to several Ohms, thus, much smaller than the characteristic impedance Z_C=50 Ohm of the transmission line. Consequently, $|2Z_L| \ll |Z_C|$, which leads to $\left|1+\frac{Z_C}{2Z_L}\right| \cong \left|\frac{Z_C}{2Z_L}\right|$. The formula given by eq. 4 can be thus simplified to:

$$S_{21} = \left|\frac{2Z_L}{Z_C}\right| \cong \frac{|Z_L|}{25} \quad \text{(eq. 6)}$$

giving

$$SE[dB] = -20\ \log_{10}\left(\frac{|Z_L|}{25}\right) \quad \text{(eq. 7)}$$

The formula expressed by eq. 7 represents thus a simplified form of eq. 4-5, valid in the case when the material under study is highly conductive. The relation between the shielding effectiveness and the electrical impedance of the material under investigation can be further developed considering the formula of Z_L and Z_C given by the eq. 1 and 2. In the case of a resistive impedance contribution Z_L=R measured at low frequencies (with negligible reactive effects), we obtain:

$$S_{21} = \left|\frac{2Z_L}{Z_C}\right| = \frac{R}{25} = \frac{1}{60\pi\sigma L} \quad \text{(eq. 8)}$$

and thus

$$SE[dB] = -20\log_{10}\left(\frac{R}{25}\right) = -20\log_{10}(60\pi\sigma L) \quad \text{(eq. 9)}$$

This equation has the same form as the DC shielding effectiveness in free space of a metallic shield [31]. A simple scaling law is revealed: an increase of one decade in the sample conductivity or in the sample thickness leads to an increase by 20 dB in the shielding effectiveness. Similarly, an increase by a factor 2 in the sample conductivity or in the sample thickness leads to an increase by 6 dB in the shielding effectiveness, while a factor of 3 increases the shielding by 9.5 dB.

3.3 The universal behavior of electromagnetic interference shielding effectiveness

In order to validate the correlation existing between shielding effectiveness and conductivity, PMMA based composite materials filled with three different types of fillers (multi-wall carbon nanotubes, carbon black, silver coated glass microfibers) were studied. Additionally, a large

collection of experimental data reported in the scientific literature, using different polymer matrices and fillers of different size, shape and nature, has been as well analyzed. With the CNT fillers, two series of samples have been prepared in our study. One series of samples was prepared by diluting a PMMA/CNT masterbatch (of 10w% CNT), upon adding additional amounts of pure PMMA into the masterbatch in order to reach a target concentration. The second series of samples has been prepared by directly adding multi-wall CNTs into the pure PMMA matrix during the melt-mixing process. The conductivity spectra of the two series of PMMA/CNT composite materials measured by BDS as a function of frequency at different filler concentrations are shown in Fig. 3.

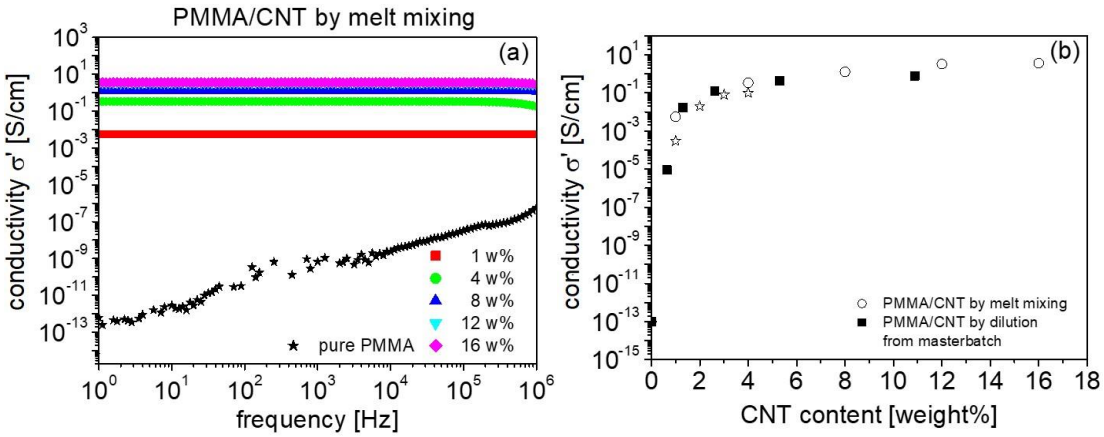

Figure 3: (a) conductivity spectra of PMMA/CNT composite materials prepared by melt mixing; (b) percolation curves (conductivity σ' as a function of filler concentration) for PMMA/CNT composite materials prepared by direct melt mixing and by masterbatch dilution. The star symbols correspond to the data reported in ref. 42.

With the increase of the amount of the CNT fillers, an increase of conductivity σ' is observed due to the phenomenon of electrical percolation [16–18,32]. Except for the pure PMMA polymer that exhibits a typical dielectric response, all the other samples show a well-defined plateau σ' that corresponds to a conductive electrical behavior. The percolation curves are presented in the Fig. 3b, by plotting the conductivity values as a function of filler concentration for both series of

samples. An identical behavior revealing a low percolation threshold of 1 wt% and equivalent conductivity values are observed. Our results are in agreement with the study McClory and Al. [21], where a comparable percolation threshold was found (1 wt%) for PMMA/CNT composite materials. They are also in agreement with the study of Logakis et al. [42], where the electrical conductivity of PMMA/CNT composite materials prepared by melt mixing was investigated. It was shown that weak polymer-filler interactions and absence of crystallinity facilitate the achievement of high conductivity values. For extending the validation of our theoretical analysis, PMMA based composite materials using other types of fillers (carbon black and silver-coated glass microfibers) were also prepared and analyzed. Their conductivity is reported in Table S1 in the Supplementary Information Part.

The morphology of the fillers, investigated by SEM, is presented in Fig. 4. The average diameter of the CNT fillers, shown in Fig. 4a, is around 15 nm, in good agreement with the value provided by the supplier. The CB fillers, presented in Fig. 4b, have an aspect ratio close to 1 and an average diameter of 60 nm. The silver-coated glass microfibers (Fig. 4c) have an average diameter of 20 microns. Their average length, measured by optical microscopy, is 109 microns.

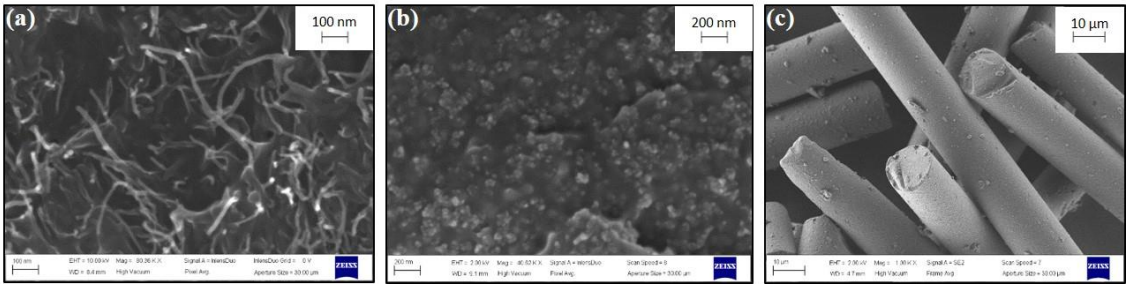

Figure 4: SEM images of the fillers used for preparing our PMMA based composite materials: (a) MWCNT; (b) CB; (c) AgGF.

The shielding effectiveness of our composite materials (PMMA/CNT, PMMA/CB, PMMA/AgGF) are presented in Fig. 5, in dependence on frequency and at different filler

concentrations. For both series of PMMA/CNT composite materials (Fig. 5a,b), significant shielding values are observed above the percolation threshold, when the samples become conductive.

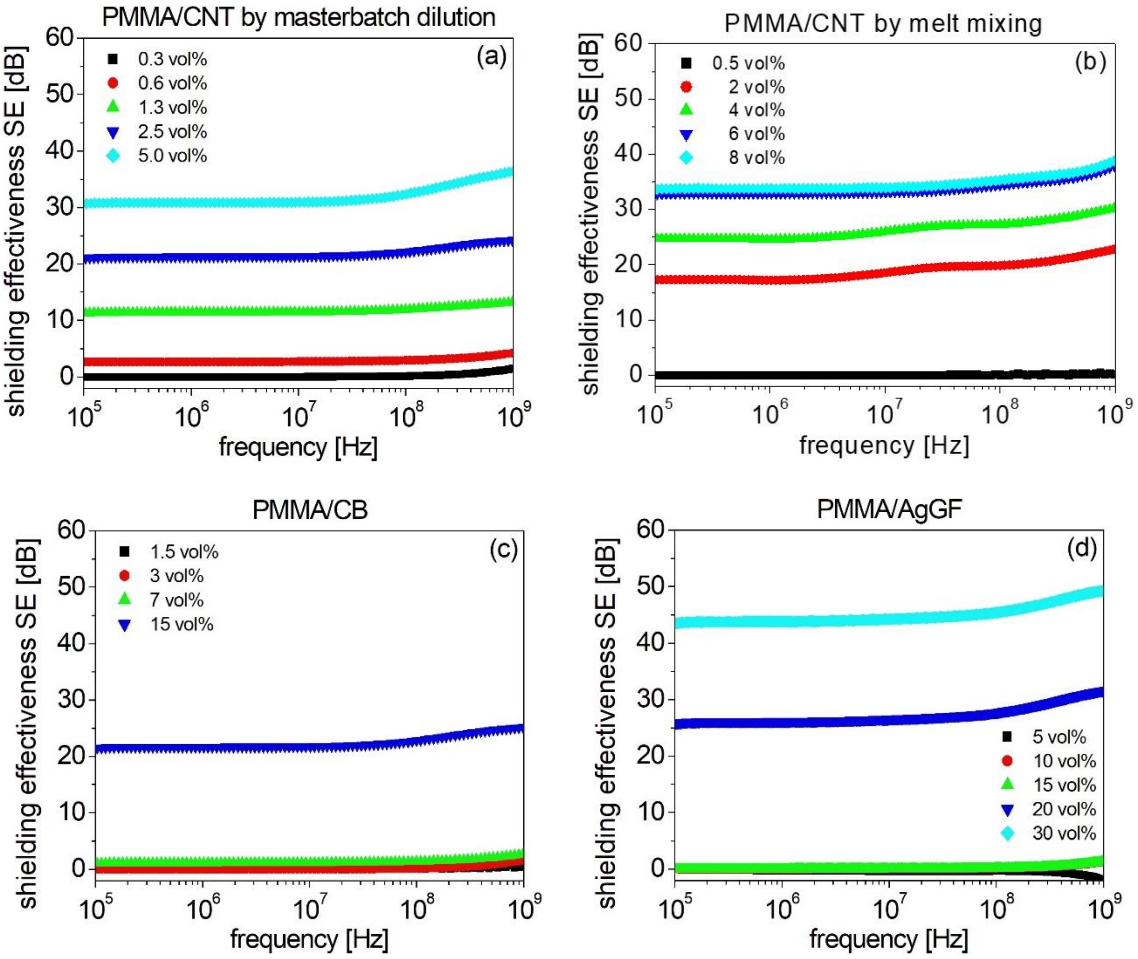

Figure 5: shielding effectiveness of (a) PMMA/CNT composite materials prepared by masterbatch dilution; (b) PMMA/CNT composite materials prepared by direct mixing; (c) PMMA/CB composite materials; (d) PMMA/AgGF composite materials, in dependence on frequency and at different filler concentrations, as indicated.

In a similar way to the conductivity behavior, the shielding effectiveness spectra of all investigated composites show constant plateau values at low frequencies. This corresponds to a shielding behavior dominated by the mechanism of simple reflection [1,2,4,7]. At high frequencies, a slight variation with the frequency is observed, which is characteristic to the onset of the shielding

mechanism by absorption [1,2]. The absorption phenomenon is basically related to the skin-depth of the investigated material but as well to the local morphology characterizing the fillers distribution. In order to extend our analysis to other types of materials, the shielding properties of gold layers have been investigated was well. Gold layers with thicknesses between 20 nm and 80 nm have been prepared by sputtering, using films of cellulose acetate and polyaramid as substrates. Their conductivity and shielding spectra are presented in the Supplementary Information Part. In the low frequency region, the composite materials investigated in the present study show thus a shielding effectiveness largely dominated by the mechanism of simple reflection, with negligible contributions due to absorption. According to our theoretical analysis (eq. 4, 5), the shielding effectiveness is essentially related to two parameters in this case: the conductivity and the sample thickness.

The correlation between the conductivity and the shielding effectiveness of all experimental data measured in our study is presented in Fig. 6a, at a frequency of 100 kHz corresponding to the shielding plateau observed at low frequencies (Fig. 5). The theoretical curve predicted by eq. 4 is shown as well, in the same graph. A broad variation in the measured conductivity, covering four orders of magnitude, is analyzed in correlation to the corresponding shielding effectiveness ranging from 0 dB to 50 dB. Materials prepared using fillers of different shape, size and nature (carbon based or metallic) show a unique "collapsing" experimental shielding curve when scaled in respect to the product between conductivity and thickness σ x d. A good agreement between the experimental points and the theoretical curve expressed by eq. 4-5 is found. The relationship revealed by Fig. 6 allows one thus a precise and absolute determination of the shielding effectiveness of materials at low frequencies by taking into consideration the value of their electrical conductivity and sample thickness. In the range where significant shielding properties are obtained (SE > 10 dB), a linear dependence between the shielding effectiveness SE and the product σ x d is revealed, in agreement with eq. 4 that gives the relationship between the transmission parameter S_{21} and the product σ x d. According to the experimental curve, an increase by one decade in the sample conductivity or thickness leads to an increase by 20 dB in the shielding effectiveness, in

agreement to the scaling law revealed theoretically. Our theoretical and experimental approach is thus confirmed for shielding measured by the coaxial method in the low frequency range and characterized by a constant shielding plateau predominantly due to reflection. The linear dependence observed at high values of σ x d in Fig. 6a,b corresponds to samples where $|2Z_L| = 2R \ll |Z_C|$=50 Ohm, thus for SE > 10 dB.

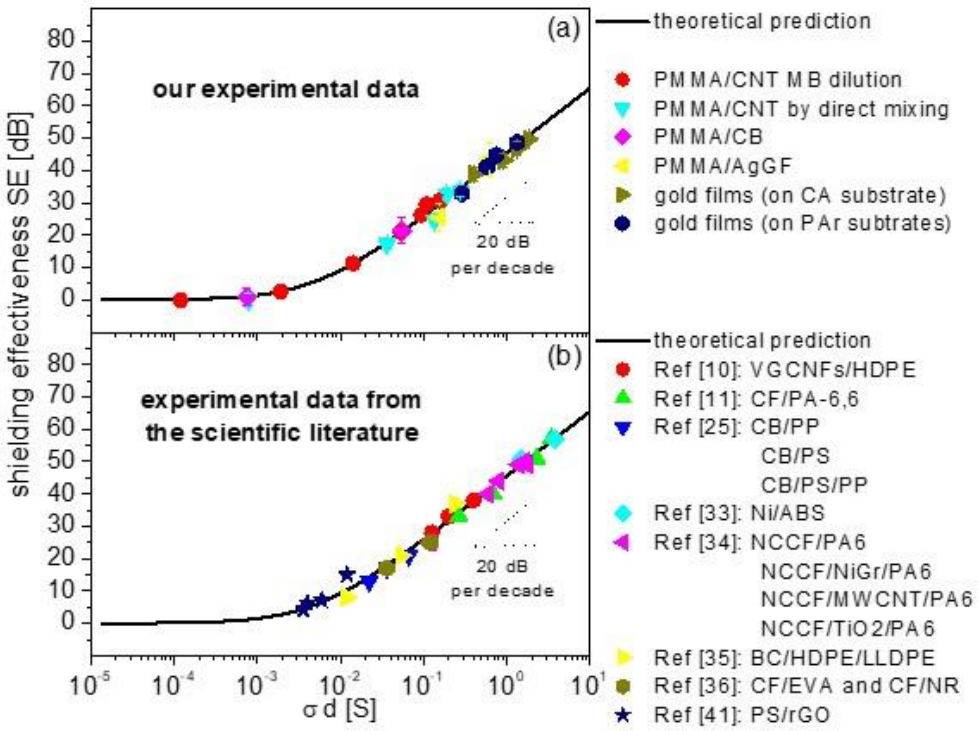

Figure 6: Shielding effectiveness as a function of the product between conductivity σ and sample thickness d for: (a) our own experimental data at 100 kHz (b) data from the scientific literature, as indicated. The continuous black lines correspond to the theoretical curve predicted by eq. 4.

The universal scaling behavior revealed in Fig. 6 can be also validated by considering the experimental data reported in the scientific literature for composite materials prepared by melt mixing and investigated by the coaxial measurement method. Different polymer matrices (high density polyethylene HDPE, polypropylene PP, polystyrene PS, polyamide PA-6, natural rubber

NR and ethylene-vinyl acetate rubber EVA, copolymer of acrylonitrile-butadiene-styrene ABS) and different types of fillers (vapor grown carbon nanofibers, carbon fibers, high structure carbon black, Nickel coated carbon fibers, Titanium Dioxide, Nickel coated graphite, biochar particles, graphene) at different filler concentrations and different sample thicknesses have been investigated [10, 11, 25, 33, 34, 35, 36, 41]. Al-Saleh et al. [10] studied the shielding properties of high-density polyethylene (HDPE) filled with vapor grown carbon nanofibers (VGCNF) at volume fractions up to 15 vol% and reported shielding effectiveness values up to 42 dB. J. M. Keith and al. [11] studied carbon fiber/Nylon 6,6 composites and obtained a maximum of 57 dB measured at 300 MHz, corresponding to a filler concentration of 40 wt%. Al-Saleh et al. [25] investigated the shielding properties of polypropylene, polystyrene and blends of polypropylene/polystyrene and polypropylene/polystyrene/styrene-butadiene-styrene filled with 10 vol% high structure carbon black. In their study, they reported that the phase segregation taking place in the PP/PS blends leads to CB fillers that are preferentially localized in the polystyrene phase, giving rise to a heterogeneous dispersion of fillers that impacts the global shielding effectiveness of their composite materials. In ref. [33], Chou et al. studied the shielding effectiveness of Acrylonitrile-Butadiene-Styrene (ABS) based composites filled with Nickel fillers (NF), in either powder or filament form. It is shown that, in the dry-mixing method, 36 dB of shielding can be obtained using only 3 vol% of nickel filaments, while much larger quantities of Ni powder are necessary in order to reach an equivalent shielding performance. T. W. Yoo et al. [34] investigated the shielding properties of polyamide 6 (PA6) based composites filled with Nickel-coated carbon fibers (NCCF) as main fillers [34] and used multi-wall carbon nanotubes (MWCNT), Nickel-coated graphite (NCG), carbon black (CB) and Titanium dioxide (TiO_2) as secondary fillers, in order to enhance the global shielding effectiveness by synergetic effects. They reported that the most efficient secondary fillers for the PA6/NCCF composites are the TiO_2 particles, due to their high dielectric constant and dominant dipolar polarization. S. Li et al. [35] reported highly filled biochar/ultra-high molecular weight polyethylene (UHMWPE)/linear low density polyethylene (LLDPE) composites with excellent

shielding properties. The biochar fillers were obtained by carbonizing bamboo charcoal (BC1100) at 1100 ^{0}C, resulting in a graphite-like structure with good electrical conductivity and high specific surface area. The addition of BC1100 enhanced the Young modulus, hardness and tensile strength of the composites but, most remarkably, significantly improved the electrical conductivity leading to excellent shielding properties. N.C. Das [36] studied the interference shielding properties of conductive rubber-based composites obtained using EVA, EPDM and 50/50 EVA/EPDM blends filled with carbon black and short carbon fibers (SCF). A higher shielding effectiveness is reported for composites based on EVA/EPDM blends as compared to composites prepared using only the pure EVA or EPDM components. This effect is related to a phase segregated morphology leading to CB fillers that are selectively localized in the EVA phase. Segregation of incompatible polymer phases leading to a selective filler distribution can be therefore a very efficient approach to enhance the shielding effectiveness of composite materials.

The experimental results reported in the scientific literature in the studies discussed above [10, 11, 25, 33, 34, 35, 36] are plotted in Fig. 6b and compared to the theoretical curve predicted by our analysis. Irrespective of the nature of the polymer matrix and that of the fillers, the experimental data collapse onto the same universal curve (Fig. 6a, b), in agreement with our theoretical prediction and our experimental data obtained on PMMA-based composites. The analysis of the experimental results reported in the literature is presented in Table 1 that gives the nature of the polymer matrix, the nature of the fillers, the sample thickness, the filler concentration, the frequency, the reported shielding effectiveness and the shielding effectiveness predicted by our theoretical analysis. A good agreement is found between the effectiveness values calculated using our theoretical approach and those experimentally measured and reported in the scientific literature [10,25,33,34]. Indeed, only a maximum deviation of 2 dB can be observed between the theoretical model and the experimental results. It is worth mentioning that the universal behavior appears to be valid also for composites showing a heterogeneous distribution of fillers, as it is the case for the phase-segregated polymer blends discussed in ref. [25, 36] where the fillers are selectively

localized in one polymer phase. One can also note that composites obtained by mixing two different (main and secondary) fillers [34] appear to follow too the prediction of our theoretical analysis.

The origin of the universal behavior reported in our study can be related to the main shielding mechanism taking place in the composite materials that were investigated. At low frequencies, all shielding materials show a shielding effectiveness that is frequency independent. This constant behavior is manifested by a plateau that can extend over many orders of magnitude in frequency up to the critical frequency where the electromagnetic absorption starts to play an important role. This frequency independent shielding characteristic to all shielding materials is the first "brick" making possible the universal behavior reported in our study. Secondly, in the frequency range corresponding to the shielding plateau, the shielding mechanism is basically entirely dominated by simple reflection, absorption effects being completely negligible. In this case, our theoretical analysis shows that the shielding effectiveness essentially depends on two parameters, the conductivity and the sample thickness, expectedly leading to the same scaling law when data are plotted as a function of these two parameters. This does not mean that shielding does not depend on composite morphology and filler distribution, but it means that, in this frequency range, any dependence of shielding on composite morphology and filler distribution arises through a change of conductivity. The structural effect on the conductivity of composites is indeed well-established in the literature, in numerous articles [37-40], and is not the goal of the current study.

In summary, our analysis reveals at low frequencies a universal scaling law governing the shielding effectiveness of composite materials in respect to the material conductivity and sample thickness. A further development in the future will attempt to systematically take into consideration also higher frequencies, also the shielding mechanisms at higher frequencies and analyze the scaling laws for shielding effectiveness spectra where both reflection and absorption take place.

Table 1: Experimentally measured shielding effectiveness values of composite materials reported in the scientific literature, where different polymer matrices and different types of fillers at

different fillers concentration (as indicated) were investigated. The experimental values are compared to the calculated shielding effectiveness values according to eq. 4.

Composites	Thickness [mm]	Filler concentration [%]	Freq.	SE exp. [dB]	SE calc. [dB]	Ref
VGCNFs/HDPE	2	15 vol%	100 MHz	38	38	[10]
VGCNFs/HDPE	2	10 vol%	100 MHz	33	32	[10]
VGCNFs/HDPE	2	7.5 vol%	100 MHz	28	27	[10]
Nickel Particles/ABS	3	25 vol%	200 MHz	51	49	[33]
Nickel Particles/ABS	3	30 vol%	200 MHz	57	55	[33]
CF/PA-6,6	3,2	15 wt%	300MHz	33	34	[11]
CF/PA-6,6	3,2	20 wt%	300MHz	40	42	[11]
CF/PA-6,6	3,2	30 wt%	300MHz	51	53	[11]
CF/PA-6,6	3,2	40 wt%	300MHz	57	56	[11]
BC/HDPE /LLDPE	2	80 wt%	300MHZ	36	34	[35]
BC/HDPE /LLDPE	2	70 wt%	300MHZ	21	20	[35]
BC/HDPE /LLDPE	2	60 wt%	300MHZ	8	7	[35]
CB/PP/PS	2	10 wt%	250 MHz	17	17	[25]
CB/PP	2	11 wt%	250 MHZ	21	22	[25]
CB/PS	2	12 wt%	250 MHZ	13	12	[25]
CF/EVA	1,8	30 wt%	500MHz	25	27	[36]
CF/NR	1,8	30 wt%	500MHz	17	17	[36]
NCCF/PA6	2	10 w%	400MHZ	25	27	[34]
NCCF/PA6	2	15 wt%	400MHZ	40	41	[34]
NCCF/PA6	2	20 wt%	400MHZ	49	48	[34]

NCCF/NiGr/PA6	2	15w%/3wt%	400MHZ	44	44	[34]
NCCF/MWCNT/PA6	2	15w%/3wt%	400MHZ	50	51	[34]
NCCF/TiO_2/PA6	2	15w%/3wt%	400MHZ	49	50	[34]

VGCNFs : Vapor grown Carbon Nanofibers, HDPE : High-density Polyethylene , ABS : Acrylonitrile Butadiene Styrene, CF : carbon Fiber, PA6-6 : Polyamide 6-6, BC : Biochar particles, LLDPE : Linear Low Density Polyethylene, CB : Carbon Black, PP : Polypropylene, PS : Polystyrene, EVA : Ethylene-vinyl acetate, NR : Natural Rubber, NCCF : Nickel Coated Carbon Fiber, PA6 : Polyamide 6, NiGr : Nickel coated graphite; MWCNT: Mutli-Walled Carbon Nanotube, TiO_2: Titanium Dioxide.

4. Conclusions

The shielding properties and the electrical properties of PMMA-based conductive composite materials using fillers of different nature (multiwall carbon nanotubes, carbon black, silver-coated glass microfibers) have been investigated in a broad frequency range, in order to systematically correlate the shielding effectiveness to conductivity and sample thickness. Our experiment approach has been corroborated with a theoretical analysis that took into count the attenuation parameter in coaxial transmission lines. At low frequencies, a universal behavior is found, all experimentally measured points falling onto a single universal curve predicted by our theoretical analysis, irrespective of the nature of the conductive materials (carbon based or metallic). This universal behavior is demonstrated not only for our own experimental results, but also for numerous experimental data reported in the scientific literature where other types of polymer matrices (high density polyethylene, polypropylene, polystyrene, polyamide, natural rubber, polyethylene-vinyl acetate and acrylonitrile-butadiene-styrene copolymer) and other types of fillers (Nickel particles, carbon fibers and nano-fibers, nickel coated carbon fibers, carbon

nanotubes) have been investigated. The good agreement between the universal behavior found in the study and our theoretical prediction opens the possibility of accurately determining the electromagnetic interference shielding performance of functional composite materials based exclusively on their electrical properties.

Acknowledgements

The financial support of the FUI project NextGen and of the Region Rhône-Alpes is highly acknowledged. The help of Laurent Cavetier in fabricating some additional metallic elements necessary for the measurements cells is kindly acknowledged.

References:

[1] C.R. Paul, Introduction to Electromagnetic Compatibility, Wiley Son. (2006).

[2] R.B. Schulz, V.C. Plantz, D.R. Brush, Shielding theory and practice, IEEE Trans. Electromagn. Compat. 30 (1988) 187–201. https://doi.org/10.1109/15.3297

[3] Meikang Han, Christopher Eugene Shuck, Roman Rakhmanov, David Parchment, Babak Anasori, Chong Min Koo, Gary Friedman, and Yury Gogotsi. Beyond Ti3C2Tx: MXenes for Electromagnetic Interference Shielding. ACS Nano 14 (2020) 5008–5016. https://doi.org/10.1021/acsnano.0c01312

[4] D.D.L. Chung, Materials for Electromagnetic Interference Shielding. Materials Chemistry and Physics 255 (2020) 123587. https://doi.org/10.1016/j.matchemphys.2020.123587

[5] M.H. Al-Saleh, W.H. Saadeh, U. Sundararaj, EMI shielding effectiveness of carbon based nanostructured polymeric materials: A comparative study, Carbon. 60 (2013) 146–156. https://doi.org/10.1016/j.carbon.2013.04.008

[6] J.-M. Thomassin, C. Jérôme, T. Pardoen, C. Bailly, I. Huynen, C. Detrembleur, Polymer/carbon based composites as electromagnetic interference (EMI) shielding materials, Mater. Sci. Eng. R Rep. 74 (2013) 211–232. https://doi.org/10.1016/j.mser.2013.06.001

[7] D.D.L. Chung, Applied Materials Science: Applications of Engineering Materials in Structural, Electronics, Thermal, and Other Industries, CRC Press LLC. (2001). https://doi.org/10.1201/9781420040975

[8] F. Qin, C. Brosseau, A review and analysis of microwave absorption in polymer composites filled with carbonaceous particles, J. Appl. Phys. 111 (2012) 061301. https://doi.org/10.1063/1.3688435

[9] S. Ganguly, P. Bhawal, R. Ravindren, N.C. Das, Polymer Nanocomposites for Electromagnetic Interference Shielding: A Review, J. Nanosci. Nanotechnol. 18 (2018) 7641–7669. https://doi.org/10.1166/jnn.2018.15828

[10] M.H. Al-Saleh, G.A. Gelves, U. Sundararaj, Carbon nanofiber/polyethylene nanocomposite: Processing behavior, microstructure and electrical properties, Mater. Des. 1980-2015. 52 (2013) 128–133. https://doi.org/10.1016/j.matdes.2013.05.038

[11] Keith Jason M., Janda Nicholas B., King Julia A., Perger Warren F., Oxby Troy J., Shielding effectiveness density theory for carbon fiber/nylon 6,6 composites, Polym. Compos. 26 (2005) 671–678. https://doi.org/10.1002/pc.20139

[12] S.H. Lee, S. Yu, F. Shahzad, J. Hong, S.J. Noh, W.N. Kim, S.M. Hong, C.M. Koo, Low percolation 3D Cu and Ag shell network composites for EMI shielding and thermal conduction, Compos. Sci. Technol. 182 (2019) 107778. https://doi.org/10.1016/j.compscitech.2019.107778

[13] J. Ju, T. Kuang, X. Ke, M. Zeng, Z. Chen, S. Zhang, X. Peng, Lightweight multifunctional polypropylene/carbon nanotubes/carbon black nanocomposite foams with segregated structure, ultralow percolation threshold and enhanced electromagnetic interference shielding performance, Compos. Sci. Technol. 193 (2020) 108116. https://doi.org/10.1016/j.compscitech.2020.108116

[14] L. Ma, W. Yang, C. Jiang, Stretchable conductors of multi-walled carbon nanotubes (MWCNTs) filled thermoplastic vulcanizate (TPV) composites with enhanced electromagnetic interference shielding performance, Compos. Sci. Technol. 195 (2020) 108195. https://doi.org/10.1016/j.compscitech.2020.108195

[15] Y. Mamunya, L. Matzui, L. Vovchenko, O. Maruzhenko, V. Oliynyk, S. Pusz, B. Kumanek, U. Szeluga, Influence of conductive nano- and microfiller distribution on electrical conductivity and EMI shielding properties of polymer/carbon composites, Compos. Sci. Technol. 170 (2019) 51–59. https://doi.org/10.1016/j.compscitech.2018.11.037

[16] S. Kirkpatrick, Percolation and Conduction, Rev. Mod. Phys. 45 (1973) 574–588. https://doi.org/10.1103/RevModPhys.45.574

[17] I. Balberg, N. Binenbaum, N. Wagner, Percolation Thresholds in the Three-Dimensional Sticks System, Phys. Rev. Lett. 52 (1984) 1465–1468. https://doi.org/10.1103/PhysRevLett.52.1465

[18] W. Bauhofer, J.Z. Kovacs, A review and analysis of electrical percolation in carbon nanotube polymer composites, Compos. Sci. Technol. 69 (2009) 1486–1498. https://doi.org/10.1016/j.compscitech.2008.06.018

[19] Y.-D. Shi, J. Li, Y.-J. Tan, Y.-F. Chen, M. Wang, Percolation behavior of electromagnetic interference shielding in polymer/multi-walled carbon nanotube nanocomposites, Compos. Sci. Technol. 170 (2019) 70–76. https://doi.org/10.1016/j.compscitech.2018.11.033.

[20] Faisal Shahzad, Mohamed Alhabeb, Christine B Hatter, Babak Anasori, Soon Man Hong, Chong Min Koo, Yury Gogotsi. Electromagnetic interference shielding with 2D transition metal carbides (MXenes). Science 353 (2016) 1137-1140. https://doi.org/10.1126/science.aag2421

[21] C. McClory, T. McNally, M. Baxendale, P. Pötschke, W. Blau, M. Ruether, Electrical and rheological percolation of PMMA/MWCNT nanocomposites as a function of CNT geometry and functionality, Eur. Polym. J. 46 (2010) 854–868. https://doi.org/10.1016/j.eurpolymj.2010.02.009

[22] N.Ch. Das, Y. Liu, K. Yang, W. Peng, S. Maiti, H. Wang, Single-walled carbon nanotube/poly(methyl methacrylate) composites for electromagnetic interference shielding, Polym. Eng. Sci. 49 (2009) 1627–1634. https://doi.org/10.1002/pen.21384

[23] M.H. Al-Saleh, U. Sundararaj, X-band EMI shielding mechanisms and shielding effectiveness of high structure carbon black/polypropylene composites, J. Phys. Appl. Phys. 46 (2013) 035304. https://doi.org/10.1088/0022-3727/46/3/035304

[24] A.A. Al-Ghamdi, O.A. Al-Hartomy, F.R. Al-Solamy, N.T. Dishovsky, P. Malinova, N.T. Atanasov, G.L. Atanasova, Correlation between Electrical Conductivity and Microwave Shielding Effectiveness of Natural Rubber Based Composites, Containing Different Hybrid Fillers Obtained by Impregnation Technology, Mater. Sci. Appl. 07 (2016) 496–509. https://doi.org/10.4236/msa.2016.79043

[25] M.H. Al-Saleh, U. Sundararaj, Electromagnetic Interference (EMI) Shielding Effectiveness of PP/PS Polymer Blends Containing High Structure Carbon Black, Macromol. Mater. Eng. 293 (2008) 621–630. https://doi.org/10.1002/mame.200800060

[26] R.K. Goyal, Cost-efficient high performance polyetheretherketone/expanded graphite nanocomposites with high conductivity for EMI shielding application, Mater. Chem. Phys. 142 (2013) 195–198. https://doi.org/10.1016/j.matchemphys.2013.07.005

[27] W.S. Jou, T.L. Wu, S.K. Chiu, W.H. Cheng, Electromagnetic shielding of nylon-66 composites applied to laser modules, J. Electron. Mater. 30 (2001) 1287–1293. https://doi.org/10.1007/s11664-001-0113-0

[28] P.F. Wilson, Techniques for measuring the electromagnetic shielding effectiveness of materials. I. Far-field source simulation., IEEE T. Electromag. C. 30 (1988) 239–250.

[29] J. Sun, W. Wang, Q. Yue, Review on Microwave-Matter Interaction Fundamentals and Efficient Microwave-Associated Heating Strategies, Materials. 9 (2016) 231. https://doi.org/10.3390/ma9040231

[30] M.H. Al-Saleh, U. Sundararaj, A review of vapor grown carbon nanofiber/polymer conductive composites, Carbon. 47 (2009) 2–22. https://doi.org/10.1016/j.carbon.2008.09.039

[31] F. Haddad, B. Bayard, B. Sauviac, Low Frequency Relation between Transfer Impedance and Shielding Effectiveness of Braided Cables and Grid Shields, IEEE Transaction on Electromagnetic Compatibility. IEEE Transactions on Electromagnetic Compatibility 62, (2020) 2423 – 2430. https://doi.org/10.1109/TEMC.2019.2960163

[32] M.H. Al-Saleh, Influence of conductive network structure on the EMI shielding and electrical percolation of carbon nanotube/polymer nanocomposites, Synth. Met. 205 (2015) 78–84. https://doi.org/10.1016/j.synthmet.2015.03.032

[33] K.-S. Chou, K.-C. Huang, Z.-H. Shih, Effect of mixing process on electromagnetic interference shielding effectiveness of nickel/acrylonitrile–butadiene–styrene composites, J. Appl. Polym. Sci. 97 (2005) 128–135. https://doi.org/10.1002/app.21740

[34] T.W. Yoo, Y.K. Lee, S.J. Lim, H.G. Yoon, W.N. Kim, Effects of hybrid fillers on the electromagnetic interference shielding effectiveness of polyamide 6/conductive filler composites, J. Mater. Sci. 49 (2014) 1701–1708. https://doi.org/10.1007/s10853-013-7855-y

[35] S. Li, A. Huang, Y.-J. Chen, D. Li, L.-S. Turng, Highly filled biochar/ultra-high molecular weight polyethylene/linear low density polyethylene composites for high-performance electromagnetic interference shielding, Compos. Part B Eng. 153 (2018) 277–284. https://doi.org/10.1016/j.compositesb.2018.07.049

[36] N.C. Das, T.K. Chaki, D. Khastgir, A. Chakraborty, Electromagnetic interference shielding effectiveness of conductive carbon black and carbon fiber-filled composites based on rubber and rubber blends, Adv. Polym. Technol. 20 (2001) 226–236. https://doi.org/10.1002/adv.1018

[37] Jie Zhang, Alexei A.Bokov, Shang-Lin Gao, Nan Zhang, Jian Zhuang, Wei Ren, Zuo-Guang Ye. Effect of hierarchical structure on electrical properties and percolation behavior of multiscale composites modified by carbon nanotube coating. Composites Science and Technology 164 (2018) 160-167

https://doi.org/10.1016/j.compscitech.2018.05.037

[38] Sai Wang, Yifeng Huang, Chongxiang Zhao, Eunse Chang, Amir Ameli, Hani E. Naguib, Chul B. Park. Theoretical modeling and experimental verification of percolation threshold with MWCNTs' rotation and translation around a growing bubble in conductive polymer composite foams. Composites Science and Technology 199 (2020) 108345

https://doi.org/10.1016/j.compscitech.2020.108345

[39] F. Cesano, M. Zaccone, I. Armentano, S. Cravanzola, L. Muscuso, L. Torre, J.M. Kenny, M. Monti, D. Scarano, Relationship between morphology and electrical properties in PP/MWCNT composites: Processing-induced anisotropic percolation threshold. Materials Chemistry and Physics 180 (2016) 284-290

https://doi.org/10.1016/j.matchemphys.2016.06.009

[40] Rudolf Hrach, Martin Švec, Stanislav Novák, Dalibor Sedlák. Electrical and morphological properties of composite films near the percolation threshold: models of composite structures. Thin Solid Films 459 (2004) 174-177

https://doi.org/10.1016/j.tsf.2003.12.133

[41] Faisal Shahzad, Seung Hwan Lee, Soon Man Hong, Chong Min Koo. Segregated reduced graphene oxide polymer composite as a high performance electromagnetic interference shield. Res. Chem. Intermed. 44 (2018) 4707–4719.

https://link.springer.com/article/10.1007/s11164-018-3274-7

[42] E. Logakis, Ch. Pandis, P. Pissis, J. Pionteck, P. Pötschke. Highly conducting poly(methyl methacrylate)/carbon nanotubes composites: Investigation on their thermal, dynamic-mechanical, electrical and dielectric properties. Composites Science and Technology 71 (2011) 854–862

https://doi.org/10.1016/j.compscitech.2011.01.029